Nano World Journal

http://dx.doi.org/10.17756/nwj.2015-005

Research Article

Open Access

Strategist PLGA Nano-capsules to Deliver siRNA for Inhibition of Carcinoma and Neuroblastoma Cell Lines by Knockdown of MYC Proto-oncogene using CPPs and PNA

Archana Raichur, Yoshikata Nakajima, Yutaka Nagaoka, Kotaro Matsumoto, Toru Mizuki, Kazunori Kato, Toru Maekawa and D. Sakthi Kumar*

Bio-Nano Electronics Research Centre, Graduate School of Interdisciplinary New Science, Toyo University, 2100, Kujirai, Kawagoe, Saitama 350-8585, Japan

***Correspondence to:**
Prof. D. Sakthi Kumar
Toyo University, Kawagoe, Saitama, Japan
E-mail: sakthi@toyo.jp

Received: February 20, 2015
Accepted: March 26, 2015
Published: April 02, 2015

Citation: Raichur A, Nakajima Y, Nagaoka Y, Matsumoto K, Mizuki T, et al. 2015. Strategist PLGA Nano-capsules to Deliver siRNA for Inhibition of Carcinoma and Neuroblastoma Cell Lines by Knockdown of MYC Proto-oncogene using CPPs and PNA. *NanoWorld J* 1(2): 32-45.

Published by United Scientific Group

Abstract

RNA interference and the therapeutic applications using small interfering RNA was discovered more than 10 years ago and currently is used in various applications including in therapeutic field. However the research in this field is still in its infancy. Many challenges like safe delivery of targeted siRNA to nucleus and cytosol of cancerous cells without compromising the activity of siRNA needs to be addressed. We have overcome this hurdle with the help of nanotechnology using PLGA hollow nanoparticles (PLGAHNPs) and suppressing the oncogene of *MYC* transcription factors by using anti myc-siRNAs in human cancer cell lines. siRNA was encapsulated in PLGAHNPs. These spherical PLGAHNPs of size 70 nm had high efficiency of gene release at pH 4.2 under *in vitro* conditions. Cell penetrating peptide (CPP)- Tat peptide (TAT) and peptide nucleic acid-nucleolus localizing signal (PNA-NLS) was used for siRNA delivery without affecting the therapeutic activity of siRNA. The siRNA duplex was prepared using T7 polymerase and double stranded DNA through *in vitro* transcription. Incubation of the siRNA encapsulated PLGAHNPs functionalized with TAT and PNA-NLS (TAT-siRNA-PNA-PLGAHNPs-siRNA) with cancer cells resulted in reduced cell proliferation. A downregulation of gene expression by 90% was observed even with low concentration of siRNA. We found complete arrest of cell division which was mediated by downregulation of *MYC* expression.

Keywords

Hollow PLGA NPs, Cell penetrating peptides, Peptide nucleic acids, siRNA delivery, Gene downregulation

Introduction

RNAi (RNA interference) therapeutics is a powerful gene therapy technique for suppressing specific genes in the cells and hence has a great potential in biomedical applications including in the treatment of genetic disorders, cancer, viral infections and autoimmune diseases [1-4]. In 1998, Andrew Fire and coworkers reported the gene silencing in the nematode *Caenorhabditis elegans* by double stranded RNA [5]. The first successful small interfering RNA (siRNA) treatment of gene silencing was achieved in hepatitis C virus. Since then gene therapy opened a new horizon for treating genetic disorders with RNAi [6]. Even though use of siRNA is effective, efficient and safe, *in vivo* delivery of siRNA to target tissues remains a key challenge for clinical implementation. As siRNA is negatively charged molecule, it is difficult to penetrate into the cell membrane [7]. Virus mediated nucleic acid delivery was adopted as an option [8]. Usually in viral delivery, very small pieces of DNA are introduced into the

cells. However, these methods are labor-intensive and expensive. Apart from this, risk of random insertion in the genome, cytophathic effects and mutagenesis are few other issues associated with viral gene delivery [9]. Therefore, viral delivery faded gradually from bioresearch field [10]. Recently, non-viral siRNA delivery systems using nanoparticles (NPs) including cationic lipids, liposomes, cationic polymers, peptide-conjugates, gold NPs, quantum dots and modified siRNA [11-18] are preferred. NPs made of polymers like polyethylenimine form conjugates with siRNA through electrostatic interactions. However, these cationic NPs have toxicity issues [19-21]. Meanwhile inorganic NPs like gold NPs and quantum dots showed great potential in siRNA delivery, researchers are still optimizing and studying the surface chemistries and investigating their long-term toxicity issues [22, 23].

Further, for the efficient use of NPs in siRNA delivery, researchers still need to overcome certain problems related to cellular uptake, degradation and renal clearance [24]. While siRNA along with the NPs were administered intravenously, they were subjected to degradation by endogenous enzymes in the blood stream. Therefore NPs should be designed in such a way that they are effective and non-toxic. Also post-injection, NP-siRNA conjugates must navigate through the circulatory system, avoiding kidney filtration, uptake by phagocytosis, aggregation with serum proteins and escape enzymatic degradation [25]. Hence, there is a need to formulate siRNA-encapsulated NPs that can target the nucleus of cancerous tissue [25-27].

Until now, biocompatible and biodegradable, PLGA NPs was used for siRNA delivery. These polymeric NPs showed enhanced encapsulation efficiency but had very low release efficiency [28]. This is because the siRNA gets entrapped in the PLGA solution during encapsulation process and its degradation takes longer time, even though PLGA is biodegradable [28]. To solve this problem we have developed PLGA hollow NPs (PLGAHNPs) that could encapsulate and efficiently release siRNA. In our previous work we showed the potential ability of PLGANPs and PLGAHNPs in drug encapsulation and release efficiency [29].

In this study, we developed a therapeutic approach using layer-by-layer (LBL) NPs to treat aggressive cancer. The advantages of LBL technique include ease of preparation, versatility, and capability of incorporating controlled high loadings of different types of biomolecules in layers. By taking advantage of this technique, we incorporated layers of Tat peptide and peptide nucleic acid-nucleolus localizing signal (PNA-NLS) on PLGAHNPs of homogenous size below 100 nm (68-70 nm). These targeting moieties layered on siRNA encapsulated PLGAHNPs enhanced the uptake of our siRNA delivery targeted cells.

Materials and Methods:

Materials

PLGA; (50:50, Mw 17000 ~ 70000), Rhodamine 6G, Fluorescein isothiocyanate isomer-I (FITC) were purchased from Sigma Aldrich, USA. Tat peptide (TAT, 49-57) of sequence (Arg - Lys - Lys - Arg - Arg - Gln - Arg - Arg - Arg) was purchased from Sigma Aldrich. PNA-NLS (H-TCAACGTTAGCTTCACC-PKKKRKV-NH_2) was purchased from PNA Bio, Inc. USA. Polyvinyl alcohol (PVA) and ethyl acetate were purchased from Kanto Chemicals, Japan. Acid yellow Tartrazine was purchased from Tokyo Chemical Industry, Japan. The linear DNA templates for siRNA synthesis, primers for β2-microglobulin, c-myc and n-myc were purchased from Eurofins, Germany. Neuroblastoma IMR-32 (CCL-127), colorectal carcinoma T84 (CCL-248) and normal cortical neuron HCN-2 (CRL- 10742) were purchased from American Type Culture Collection, USA. Ambion siRNA construction kit, Life technology, Japan was used for the synthesis of siRNA and quantified using Ribogreen reagent (Qubit™ RNA Assay Kits, Invitrogen, Japan). For cell proliferation study, MTS-based colorimetric assay (Cell titer 96 AQ One Cell Proliferation assay, Promega Corporation's, USA) was used. Alexa Fluor® 488 annexin V/ Dead Cell Apoptosis Kit (Invitrogen) was used for studying apoptosis. RNeasy Mini kit (Qiagen) was used for isolation of mRNA. One Step SYBR PrimeScript PLUS RT-PCR Kit (Takara Bio Inc) was used for qRT-PCR.

Synthesis of PLGA Hollow nanoparticle preparation (PLGAHNPs)

Hollow nanoshells were synthesized as described in our previous paper [29], using simple solvent emulsion evaporation method. Briefly 50 mg of PLGA was dissolved in 1ml of ethyl acetate. This solution was vortexed for one hour. The above vortexed PLGA solution was emulsified in 5% (w/v) of 2 ml of PVA solution. This solution was stabilized in 0.05% (w/v) PVA solution to form colloidal solution containing PLGAHNPs.

siRNA duplex preparation

The silencer siRNA used in the experiment, corresponding to sequence 447 - 449 relative to the start codon of c-myc Gene bank Accession no. AA149343 and sequence 997 - 998 of n-myc mRNA sequences Gene Bank Accession no. X03294 were synthesized after *in vitro* transcription and hybridization of the sense and antisense strands. siRNA synthesis was carried out according to the manufacturer's instruction. Briefly, the siRNA duplexes were synthesized by *in vitro* transcription with T7 RNA polymerase on linear DNA templates selecting part of mRNA reference sequences from human n-myc and c-myc. The DNA strands designed and used for synthesizing siRNA were:

c-myc

sense DNA 5'-AATAATTGGCCCAAGTCATTG-CC-TGTCTC-3'

antisense DNA 5'-AACAATGACTTGGGCCAAT-TA-CCTGTCTC-3'

n-myc

sense DNA 5'-AAGTCAAACTCGAGGTCTGGG-CCT-GTCTC-3'

antisense DNA 5'-AACCCAGACCTCGAGTTT-GAC-CCTGTCTC-3'

The above 29-mer DNA oligonucleotides (template oligonucleotides) with 21 nucleotides (nt) encoding siRNA and 8 nt complementary to the T7 Promoter Primer

were synthesized. In separate reactions, the two template oligonucleotides were hybridized to a T7 Promoter Primer that is provided in the kit that contains a T7 promoter sequence. The 3' ends of the hybridized DNA oligonucleotides were extended by the Klenow fragment of DNA polymerase to create double-stranded siRNA transcription templates. The sense and antisense siRNA templates were transcribed by T7 RNA polymerase and the resulting RNA transcripts were hybridized to create dsRNA. The dsRNA consisted of 5' terminal single-stranded leader sequences, a 19 nt target specific dsRNA, and 3' terminal UUs. The leader sequences are removed by digesting the dsRNA with a single strand specific ribonuclease supplied in the kit. Overhanging UU dinucleotide remained on the siRNA and this helped in further transfection. The DNA template is removed at the same time by a deoxyribonuclease. The resulting siRNA is purified by elution method, which removes excess nucleotides, short oligomers, proteins and salts in the reaction mixture. The end product is a double-stranded 21-mer siRNA with 3' terminal uridine dimers that can effectively reduce the expression of target mRNA when transfected into mammalian cells.

Our siRNA sequences were designed according to the guidelines by Ui-Tei et al. [30] and homology to other genes were confirmed using BLAST. The molarity and concentration of siRNA prepared were calculated according to the instructions in user manual for siRNA synthesis.

Preparation of siRNA encapsulated PLGA NPs

siRNA encapsulated PLGA NPs were synthesized using the simple solvent emulsion evaporation method. In brief, different concentration of siRNA ranging from 100, 500, 1000, 1500, 2000 and 2500 µg/ml solubilized in Tris–EDTA buffer (10 mM Tris, 1 mM EDTA, pH 7.5, TE buffer) were mixed with 3 mg of PLGA and 60 µl of ethyl acetate in a closed vial and was emulsified to synthesize siRNA encapsulated PLGAHNPs. The NPs were collected by centrifugation at 10000 rpm for 8 min and these NPs were further washed with 5 ml of diethylpyrocarbonate (DEPC)- treated water, vacuum dried and stored at -80 °C till further use.

siRNA encapsulation was done according to the protocol reported by Cun et al. [31] 2 mg each of NPs containing different concentrations of siRNA was dissolved in 200 µl of chloroform and 500 µl of TE buffer. This mixture was rotated for one hour, and the phases were separated by centrifugation for 30 min at 12000 rpm at 4 °C. The supernatant was kept at room temperature for 5 min for complete evaporation of chloroform. The samples were diluted in TE buffer and concentration of siRNA was measured by Ribogreen reagent. Readings were taken using plate reader at excitation wavelength of 485 nm and emission wavelength of 520 nm. Each sample was assayed in triplicates and the following equations were used to calculate the amount of siRNA encapsulated.

$$\epsilon_{siRNA\ Ld} = \frac{W_{siRNA}}{W_{NPs}} \quad \text{....(1)}$$

Where

$\epsilon_{siRNA\ Ld}$ = siRNA loading

W_{siRNA} = The weight of siRNA in NPs

W_{NPs} = The weight of NPs

$$\epsilon_{\%\ EE} = \frac{E_{siRNA\ E\ ncap.}}{E_{\text{siRNA Used}}} \times 100 \quad \text{.....(2)}$$

Where

$\epsilon_{\%\ EE}$ = % Encapsulation efficiency

$E_{siRNA\ E\ ncap.}$ = Actual amount of siRNA encapsulated in NPs

$E_{\text{siRNA Used}}$ = The amount of siRNA used for encapsulation

Release of siRNA

The release of siRNA was determined from PLGAHNPS using UV-Vis spectrophotometer. 10 mg of siRNA encapsulated PLGAHNPs was suspended in 10 ml each of Tris-HCl buffer of pH 7.4 and 4.2. Further they were filtered through 0.45, 0.25 and 0.15 µm pore sized Whatman filters to obtain NPs ranging from 50 - 400 nm. Further, aliquots of 1 ml of the above solutions were prepared and placed on a rotator with a stirring speed of 100 rpm at 37 °C for 72 h. At specific time intervals (0, 2, 4, 6, 12, 24, 36, 48, 60 and 72 h) samples were centrifuged at 14000 rpm for 8 min at 4 °C. Then, the supernatant was used to estimate the amount of siRNA released from HNPs by qualitatively analyzing the concentration of siRNA at 260 nm [32, 33]. Each sample was assayed in triplicates and the release efficiency was determined.

Preparation of functionalized PLGA HNPs

The synthesized siRNA encapsulated PLGAHNPs were functionalized with TAT and PNA-NLS for studying anticancer activity in two different cancer cell lines- IMR-32 and T84, and normal cell line HCN-2. 1 mg of siRNA encapsulated PLGAHNPs was functionalized with PNA-NLS and TAT peptide. Two types of functionalized NPs were prepared, a) siRNA encapsulated PLGAHNPs-coated-PNA-NLS (PAPLGAHNPs), b) TAT peptide coated over siRNA-PNA-NLS-siRNA encapsulated PLGAHNPs (TPAPLGAHNPs) The reason behind coating TAT on PAPLGAHNPs was to increase cell permeability.

PNA-coated NPs were developed by incubating 1 mg of PLGAHNPS in 1, 2.5, 5, 10, and 20 µmol/L of PNA-NLS dissolved in 10 mM Tris buffer (pH 8) for 4 h at room temperature. After incubation, PLGA-PNA NPs were collected by centrifugation at 8000 rpm for 30 min at 4 °C. They were resuspended again in fresh PNA solution and incubated on ice for an additional 3 h without rotation. These PNA-PLGA NPs were collected by centrifugation at 8000 rpm for 20 min at 4 °C and were resuspended in fresh deionized water. These synthesized PAPLGAHNPs were rotated for 20 min prior to experiment. For the preparation of PLGA-PNA-siRNA conjugates, the above prepared NPs were suspended in anti-n-myc and anti-c-myc siRNA of different concentrations (70 nM and 80 nM) with 10 mM of NaCl and 1 mM Tris buffer of pH 7.4 for 20 min at room temperature. After incubation the particles were collected by centrifugation at 5000 rpm for 10 min at 4 °C. Further, for preparation of

TAT-siRNA-PNA-PLGAHNPs conjugates, the above prepared siRNA-PNA-PLGANPs were incubated in 1mM PBS containing TAT with concentration of 10, 50, 100 and 150 µg/ml at room temperature and kept for rotation. The functionalized NPs were collected by centrifugation at 8000 rpm for 10 min [34-36].

Preparation of fluorescently labeled NPs

Two types of fluorescently labeled NPs were prepared for studying the cellular and nuclear uptake. As we wanted to determine the site specificity and accumulation of NPs, we used PNA-NLS and TAT to target the cells. The first type of fluorescent PNA-PLGAHNPS (PAPHNPs) were prepared by conjugating Rhodamine - PNA complex on Tartrazine-siRNA encapsulated PLGAHNPS complex. 20 µmol/L PNA-NLS was added to 5 mM of Rhodamine and incubated for 1 h. 1 mg of siRNA-PLGAHNPs of approximately 70 nm was incubated with 20 mM of Tartrazine. Both complexes were mixed in Tris buffer and incubated on ice for 7 h. Resulting PAPHNPs were collected by centrifuging the above solution at 3000 rpm for 10 min at 4 °C

The second type of fluorescently labeled TAT-siRNA-PNA-PLGAHNPS (TPAPHNPs) was prepared by incubating siRNA-PAPHNPs in 0.5 mM of FITC-DMSO-TAT solution. TAT-FITC was prepared on ice by incubating

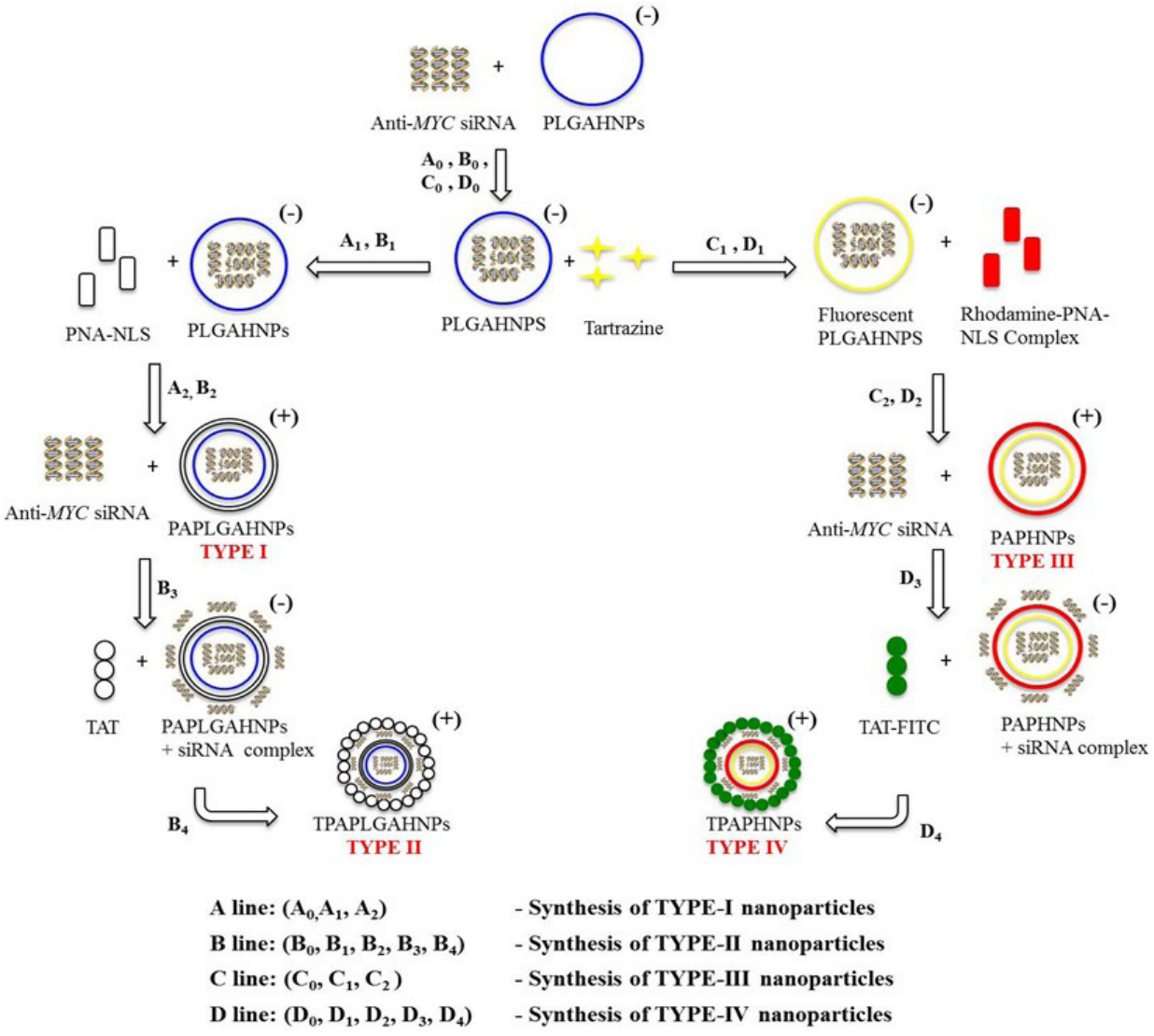

Figure 1: Schematic representation of synthesis of four types of anti-myc-siRNA encapsulated PLGA nanoparticles.

Notes: A line: Synthesis of non-fluorescent Type I PAPLGAHNPs wherein A_0 represents the encapsulation of siRNA to form PLGAHNPS, A_1 is incubation of PNA-NLS with anti-MYC siRNA encapsulated PLGAHNPs and A_2 is formation of TYPE-I nanoparticles "PAPLGAHNPS".

B line: Synthesis of non-fluorescent Type II TPAPLGAHNPs wherein B_0 represents the encapsulation of siRNA to form PLGAHNPS, B_1 is incubation of PLGAHNPS with PNA-NLS to form PAPLGAHNPS, B_2 is incubation of PAPLGAHNPS with anti-MYC-siRNA to form siRNA layered PAPLGAHNPS, B_3 is incubation of PAPLGAHNPS with TAT peptide and B_4 is formation of TYPE-II functionalized nanoparticles of "TPAPLGAHNPS".

C line: Synthesis of Type II nanoparticles wherein C_0 represents the encapsulation of siRNA to form PLGAHNPS, C_1 is incubation of PLGAHNPS with tetrazine to form negatively charged fluorescent nanoparticles, C_2 is incubation of these nanoparticles with Rhodamine 6G-PNA-NLS complex to form TYPE-III positively charged fluorescent nanoparticles of "PAPHNPs".

D line: Synthesis of Type IV fluorescent nanoparticles wherein D_0 represents the encapsulation of siRNA to form PLGAHNPS, D_1 is formation of PLGAHNPS, D_2 is formation of PAPHNPs, D_3 is incubation of PAPHNPs with siRNA to form negatively charged siRNA layered PAPHNPs, D_4 is incubation of FITC tagged TAT peptide with siRNA layered PAPHNPs to form polycation of TYPE-IV "TPAPHNPs".

TAT peptide and FITC-DMSO solutions for 20 min. These NPs were washed in deionized water to remove excess FITC and the NPs were collected and resuspended in deionized water for further studies.

Technically, four types of siRNA encapsulated PLGAHNPs namely a) PAPLGAHNPs b)TPAPLGAHNPs (non-fluorescent NPs), c) PAPHNPs and d) TPAPHNPs (fluorescent NPs) moieties were synthesized as represented in figure 1 for studying the *in vitro* effects on cancer cells. Cell proliferation ability, mode of cell death, uptake of NPs in cancer cells and downregulation of MYC-gene were studied. These NPs were stored at -20 ˚C till further use.

Characterization of NPs

The NPs (1 mg/ml) were suspended in deionized water and were characterized for their shape and size using Scanning Electron Microscopy (SEM, JEOL, JSM-7400F) and Transmission Electron Microscopy (TEM, JEM 2100, JEOL). SEM was performed at 5 kV and TEM at 180 kV. Zeta potential and Dynamic Light Scattering (DLS) of PAPLGAHNPs, TPAPLGAHNPs, PAPHNPs and TPAPHNPs were analyzed using Malvern Zetasizer Nano.

Cell culture

Monolayer of IMR-32 and T84 were maintained within 1-8 passages [37, 38]. IMR-32 cells were cultured for 3 days in Eagle's Minimum Essential Medium (EMEM), with 10% of heat inactivated fetal bovine serum (FBS) and antibiotics. The T84 cells was cultured for 5 days to get a monolayer in Dulbecco's Modified Eagle's Medium (DMEM) - Ham F12K media with 5% serum and antibiotics. The HCN-2 cells were cultured and maintained in DMEM, with 10% FBS and antibiotics. For studying the cell proliferation, flow cytometry and relative mRNA expression level, these cells were grown to confluency with a viability of 85 – 99%. The viability of the cells was checked using trypan blue assay.

Analysis of cell proliferation

IMR-32, T84 and HCN-2 cells were seeded in 96-well culture plates ($5x10^4$ cells/well) and treated with different concentration of NPs containing various concentrations of siRNA and were incubated overnight. MTS-based colorimetric assay was used for cell proliferation study, where PAPLGAHNPs and TPAPLGAHNPs containing different concentrations of anti- c-myc and anti-n-myc siRNA (50, 70, 80 nM) were used. The absorbance was measured at 490 nm [39].

Flow cytometry

The mode of cell death and effect of the functionalized NP on the cells were confirmed by flow cytometry. The cells were seeded at a concentration of 5×10^3 cells/well in 6-well plates and treated with functionalized NPs. IMR-32 cells were incubated overnight with 200 µg/ml each of TPAPLGAHNPs and PAPLGAHNPs keeping 70 nM of anti-n-myc siRNA in PLGAHNPS. While 150 µg/ml of TPAPLGAHNPs and 250 µg/ml of PAPLGAHNPs with concentration of 80 nM of anti-c-myc siRNA were treated with T84 cells. The HCN-2 cells were incubated with 200 µg/ml (70 nM of anti-n-myc siRNA) and 150 µg/ml (80 nM of anti-c-myc siRNA) of TPAPLGAHNPs; 200 µg/ml (70 nM of anti-n-myc siRNA) and 250 µg/ml (80 nM of anti-c-myc) of PAPLGAHNPs. The cell death was observed in both the cancer cells using live and dead cell assay kit. Flow cytometry measurements were taken at fluorescence emissions of 530 nm and 575 nm [40]. Same procedure was carried on normal cells to determine the effect of NPs.

Cellular uptake of NPs

To investigate the site targeted delivery and accumulation of the NPs, HCN-2, IMR-32 and T84 cells were incubated with fluorescent PAPHNPs and TPAPHNPs. Two sets of each type of cell lines were plated on a 35 mm glass base confocal plate till the cells reached 70-80% confluency. One set of each cell type was kept for 4 h uptake studies and another set for overnight observation. Hoechst 33342 nucleic acid stain was used for staining nucleus. 4 h after the treatment, one of the above sets containing control and treated cells were washed with Dulbecco's Phosphate Buffered Saline (DPBS), fixed by 4% formaldehyde solution in DPBS for 10 min and stained with Hoechst 33342 in DPBS for 20 min for nucleus visualization. The cells were washed twice with DPBS and images were obtained using confocal microscopy. The laser of 405, 488, 561 and 640 nm were used to accquire the images. The other set was incubated overnight for observation of effect of NPs. The fluorescence signals were quantified and efficacy of the nanoparticle's accumulation was measured using the formula [41]:

$$\frac{G}{B} = \frac{\left(\frac{Gcell}{Scell} - \frac{Gbgr}{Sbgr}\right)}{\left(\frac{Bcell}{Scell} - \frac{Bbgr}{Sbgr}\right)} \quad \ldots.(3)$$

Where

G- green fluorescence signal from FITC

B - blue signals from Hoechst

Gcell, Bcell- green and blue signal intensities in the cells

Scell - square of cell area where the fluorescent signal is measured

Sbgr- square of the background area

Gbgr, Bbgr- background green and blue signals intensities

Uptake in nucleus

Nuclear uptake of the NPs was confirmed by confocal microscopy. Cells were incubated with functionalized fluorescent NPs (TAT-anti *MYC* siRNA-PNA-NLS-PLGAHNPs) for 4 h. The 3D reconstruction of *in vitro* cultures was carried out to investigate the accumulation and nucleus targeting specificity of NPs that were present in and around nucleus [42].

Morphologic analysis

HCN-2, IMR-32 and T84 cells were cultured for 3 days in six well plate containing PAPLGAHNPs and TPAPLGAHNPs. Phase contrast microscopy was used to check the morphological changes in cells after co- incubation with the NPs.

RNAi treatment

Investigation of gene inhibition was studied on HCN-2, IMR-32 and T-84 cells. The cells were grown to confluency and

treated with 250 µg/ml (70 nM of anti-n-myc siRNA) and 150 µg/ml (80 nM of anti-c-myc siRNA) of TPAPLGAHNPs; 250 µg/ml (70 nM of anti-n-myc siRNA) and 350 µg/ml (80 nM of anti-c-myc siRNA) of PAPLGAHNPs. Cells were treated and incubated overnight for two days with NPs. The cells were then harvested to check n-myc and c-myc mRNA expression by qRT-PCR [43].

Relative gene expression studies using qRT-PCR

Cells were harvested and washed with DPBS. Total RNA was isolated from these cells using RNeasy Mini kit and quantified by UV spectrophotometry [43]. Complementary DNA (cDNA) was prepared from 1.56 µg of total cellular RNA using oligo-dT18 primers according to the manufacturer's protocol. Relative gene expression of c-myc, n-myc mRNA were compared with that of human β2-microglobulin mRNA was determined by qRT-PCR.

Following primers were used:

c-myc forward: 5'-CTCCTCGGTGTCCGAG- GACC-3';

c-myc reverse: 5'-GTTCGCCTCTTGACA-TTCTCC-3';

n-myc forward: 5'-TCTGTCGGTTGCA-GTGTTG-3';

n-myc reverse: 5'-TTCTCAAGCAGG-ATCTCCG-3';

β2-microglobulin forward:
5'-ATCTTCAAACCTCCATGATG-3'

β2-microglobulin reverse:
5'-ACCCCCACTGAAAAAGATGA-3'

The concentration of mRNA used was 10 µM, with 1 µl primer mix (sense and antisense) in 25 µL q-PCR reaction mixture. The q-PCR was performed using One Step SYBR PrimeScript PLUS RT-PCR Kit based on the manufacturer's protocol after optimization. Inhibition of c-myc and n-myc mRNA was determined by comparison of the ratio between c-myc and n-myc, and β2-microglobulin mRNA for the treated groups against the untreated group. RT-PCR products were subjected to electrophoresis on 2% agarose gel and visualized by ethidium bromide staining. Agarose gel was photographed and intensities were determined using BioRad GS710. The standard curve obtained from PCR showed the level of mRNA concentration present in the treated and non-treated cells. We have calculated the relative mRNA expression by using the equation 4.

$$E = (10^{-1/slope} - 1) \times 100 \quad \ldots(4)$$

Results

Nanoparticle characterization

SEM, TEM and DLS were used to characterize the NPs. Figure 2A represents the SEM image of PLGAHNPs that were spherical in shape and hollow. In TEM image (Figure 2B), we observed the absence of inner core in the NPs. Compared to figure 2B, in figure 2C we could observe the presence of light shadow region, depicting the presence of siRNA encapsulated in the hollow NPs. According to the DLS (Figure 2D) the mean diameter of siRNA encapsulated PLGAHNPs was around 70 nm after it was filtered through 0.15 µm Whatman filter.

siRNA encapsulation efficiency

The encapsulation efficiency of siRNA into NPs plays a significant role in "non-viral gene delivery". It is reported that the encapsulation efficiency of non-hollow PLGANPs

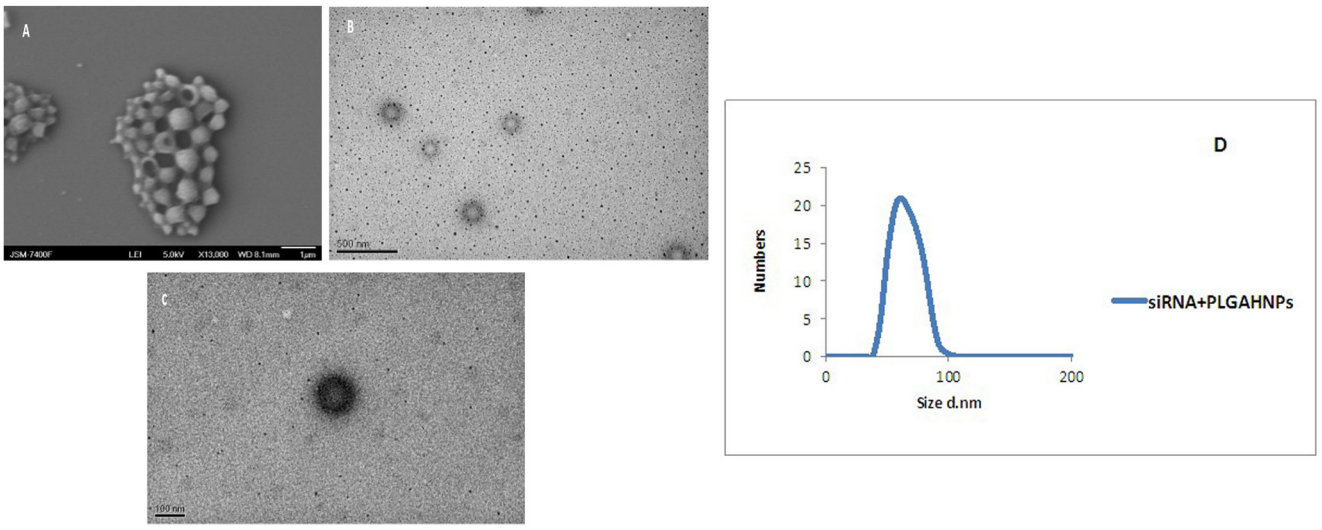

Figure 2: Characterization of PLGAHNPs and siRNA encapsulated PLGAHNPs.

Notes: A: SEM of PLGAHNPs. B and C: TEM images of PLGAHNPs and siRNA encapsulated PLGAHNPs. D: DLS of siRNA encapsulated PLGAHNPs

Abbreviations: PLGAHNPs- PLGA hollow nanoparticles, SEM-Scanning electron microscope, TEM-Transmission electron microscope, PLGAHNPS- siRNA encapsulated PLGA hollow nanoparticles.

is affected by the concentration of PLGA used to synthesize the NPs [31, 44]. We have used PLGAHNPs to encapsulate higher amount of siRNA and protect it from degradation. From figure 3 the amount of siRNA encapsulated was 1997 ± 0.76 µg/ml when 2000 µg/ml of siRNA was used for encapsulation. The efficiency of siRNA encapsulation was 99 ± 0.42% as calculated using equation 2.

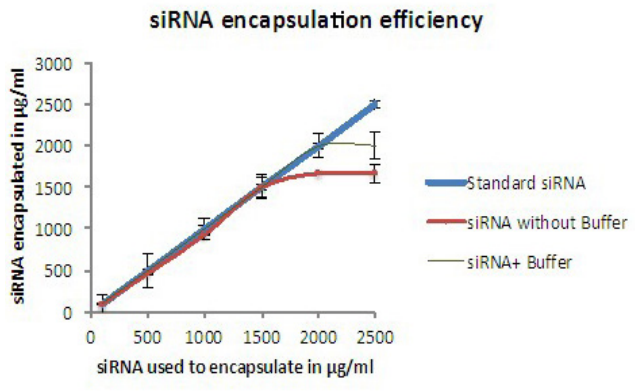

Figure 3: siRNA encapsulation efficiency of PLGAHNPS.

Notes: Graph showing siRNA encapsulation efficiency of PLGAHNPS. 1997±0.7 µg/ml of siRNA was encapsulated when 2000µg/ml of siRNA with buffer was used.

Abbreviations: PLGAHNPS-PLGA hollow nanoparticles encapsulated in PLGAHNPs

siRNA release efficiency

PLGA NPs favor siRNA delivery systems because they can readily be surface-modified to enhance targeting or cellular uptake [45]. We found that PLGAHNPs show efficient encapsulation and *in vitro* release of siRNA and have the capacity to protect the siRNA from the external environment. In our experiment the PLGA HNPS were filtered through 0.45, 0.25 and 0.15 µm sized Whatman filters. As shown in figure 4A we obtained NPs of mean size around 260 ± 0.49, 105 and 70 ± 0.77 nm respectively after filtering. Further from graph in figure 4B and C we concluded that the maximum siRNA release is from 70 nm sized PLGAHNPS when compared to other larger PLGAHNPS. Maximum amount of siRNA release in pH 7.4 was 1786 µg/ml, and the release efficiency was 89 ± 0.89%. The siRNA release from other NPs was comparatively lower (78% for 105 nm and 0.00015% for 260 ± 0.49 nm). From figure 4C we observed that the NPs of 70 nm showed 94% of siRNA release after 12 h in pH 4.2 and sustained release after 12 h. We performed siRNA release in pH 4.2 to mimic the acidic environment of endosomes in the cells [29, 31].

At pH 4.2 the release efficiency of 105 nm was 84% and of 260 ± 0.49 nm was $4x10^{-4}$%. For further studies with targeting moieties, NPs of size 70 nm were selected. The size, siRNA encapsulation and release efficiency was suitable for siRNA delivery in cancer cells. It is reported that the NPs of size ranging from 70-200 nm are best suited for *in vitro* and *in vivo* delivery [46].

Characterization of functionalized NPs

TAT and PNA-NLS were attached to the surface of siRNA (anti-c-myc and anti-n-myc) encapsulated PLGAHNPS by layer-by-layer assembly. After the incubation and addition of targeting moieties, hydrodynamic size and zeta potential were analyzed. We observed that the targeting moieties formed a layer on the HNPs. Figure 5 showed the SEM image of these functionalized NPs.

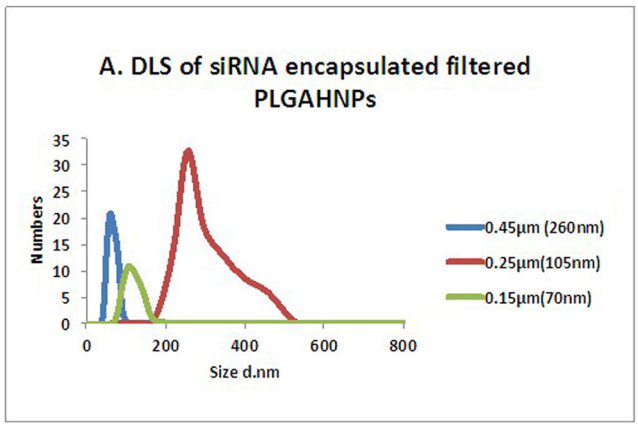

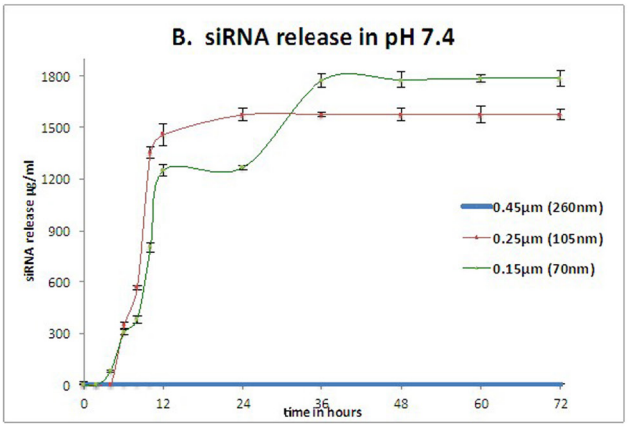

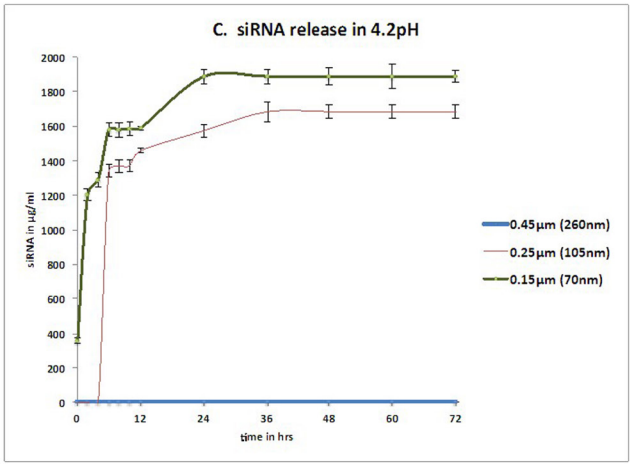

Figure 4: DLS of PLGAHNPS after filtering and siRNA release efficiency of PLGAHNPS (0.45µm, 0.25µm and 0.15 µm are the filters used.

Notes: (A) Graph presenting mean size of filtered siRNA encapsulated PLGAHNPS. (B) and (C): Graph of siRNA release from PLGAHNPS in pH 7.4 and 4.2, respectively.

Abbreviation: PLGAHNPS-siRNA encapsulated nanoparticles; PLGAHNPs-PLGA hollow nanoparticles

Table 1 summarizes surface charge, size and encapsulation efficiency of PLGAHNPS, PAPLGAHNPs, TPAPLGAHNPs, PAPHNPs and TPAPHNPs. The size of PLGAHNPS increased from 58 nm to 123 ± 0.87 nm after functionalizing with targeting moieties to form TPAPLGAHNPs. The functionalized fluroscent NPs were larger in size than non-fluroscent NPs. The surface charge of PLGA NPs without fluorescent moiety was -7 mV. After conjugation of PNA and TAT peptide, the surface charge was +12 and +29 mV respectively, suggesting the formation of peptide layer on PLGAHNPS. A layer of anti-c-myc and anti-n-myc siRNA was inserted in between two peptides. This contributed an increase in hydrodynamic size and decrease in surface charge to -5 mV after the formation of PNA layer. Although the TAT layer increased the size, the surface charge was maintained to +29 mV creating cationic TPAPLGAHNPs, which made the penetration into the cell membrane easy [35, 47]. The targeting moieties converted the PLGAHNPs to cationic polymeric NPs, which made them ideal carriers for gene delivery [47]. Thus after the complete functionalization of PLGAHNPS, the cellular and nuclear uptake were studied in different cell lines.

Effect of NPs on cell

The minimum inhibitory concentration (MIC) required for inhibiting cell proliferation was determined using MTS assay. Cancer cells were treated with different molar concentrations of anti-*MYC*-siRNA (anti-n-myc siRNA for IMR-32 cells and anti-c-myc siRNA for T84) ranging from 50 - 90 nM. From figure 6B, D and F we can observe the effect of optimized molar concentration of anti-*MYC*-siRNA on IMR-32, T84 and HCN-2. 70 nM of anti-n-myc siRNA was optimized as MIC required for inhibiting IMR-32 cells and 80 nM of anti-c-myc siRNA was required to inhibit T84 cells. There was no significant effect on proliferation observed in HCN-2 cells. Further we treated IMR-32, T84 and HCN-

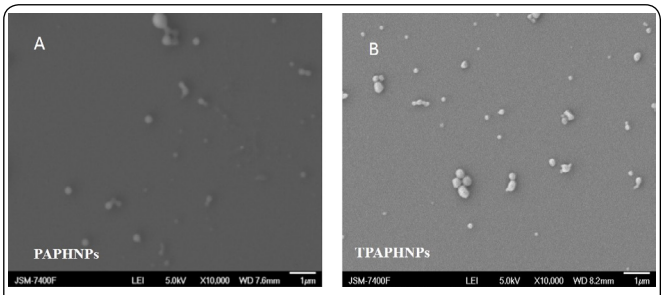

Figure 5: SEM images of functionalized siRNA encapsulated PLGA hollow nanoparticles.

Notes: Left image represents the PLGAHNPS functionalized with PNA-NLS only. Right image represents PLGAHNPS functionalized with TAT peptide, siRNA and PNA-NLS.

Abbreviations: PLGAHNPS-siRNA encapsulated PLGA hollow nanoparticles

Table 1: Particle size, zeta potential, siRNA loading of PLGA HNPS. Data is expressed as averages (Standard deviation) of 2-9 identically but independent samples

Nanoparticles	Properties of NPs				siRNA Encapsulation efficiency (%)
	Nont-Fluorescent (Blank)		Fluorescently Labeled		
	Size (nm)	Zeta potential (mv)	Size (nm)	Zeta potential (mv)	
PLGA	58.57	-7.06	69.06	-15.04	93.45
PLGA+PNA-NLS	78.82	16.2	91.28	12	96.05
PLGA+PNA-NLS +siRNA (c-myc)	105	-2.51	113.3	-5.88	96.00
PLGA+PNA-NLS +siRNA (n-myc)	115	-0.3	121	-1.7	96.00
PLGA+PNA+NLS +siRNA+TAT (c-myc)	121.2	25.3	122	29.5	96.00
PLGA+PNA+NLS +siRNA+TAT (n-myc)	123.87	11.5	124.06	15.7	96.00

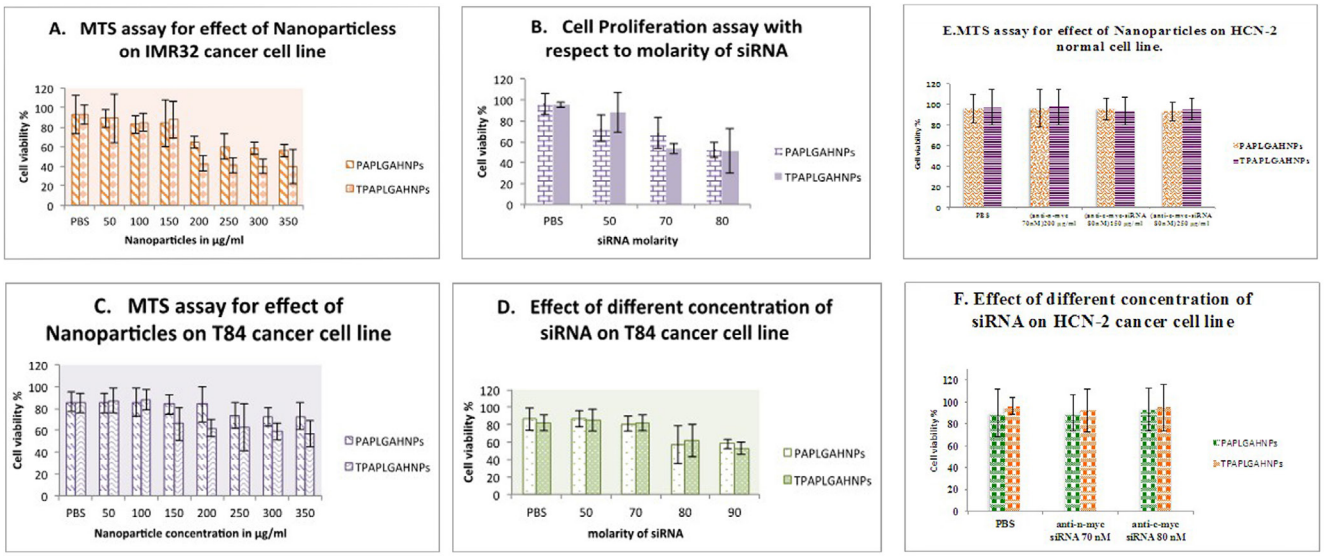

Figure 6: Effect of functionalized nanoparticles on cancer cell proliferation and normal cell proliferation.

Notes: Untreated cells were used as negative control. From graph B and D, the inhibitory concentration of siRNA was 70nM and 80nM. A and C: Cell viability following incubation with PAPLGAHNPs and TPAPLGAHNPs for overnight. E and F: Effect of functionalized nanoparticles on normal HCN-2 cells. Results are presented as the mean of the three measurements ± standard deviation.

Abréviations: PAPLGAHNPs- PNA layered on PLGA-siRNA encapsulated hollow nanoparticles, TPAPLGAHNPs- TAT, siRNA, PNA layered on PLGA- siRNA encapsulated hollow nanoparticles.

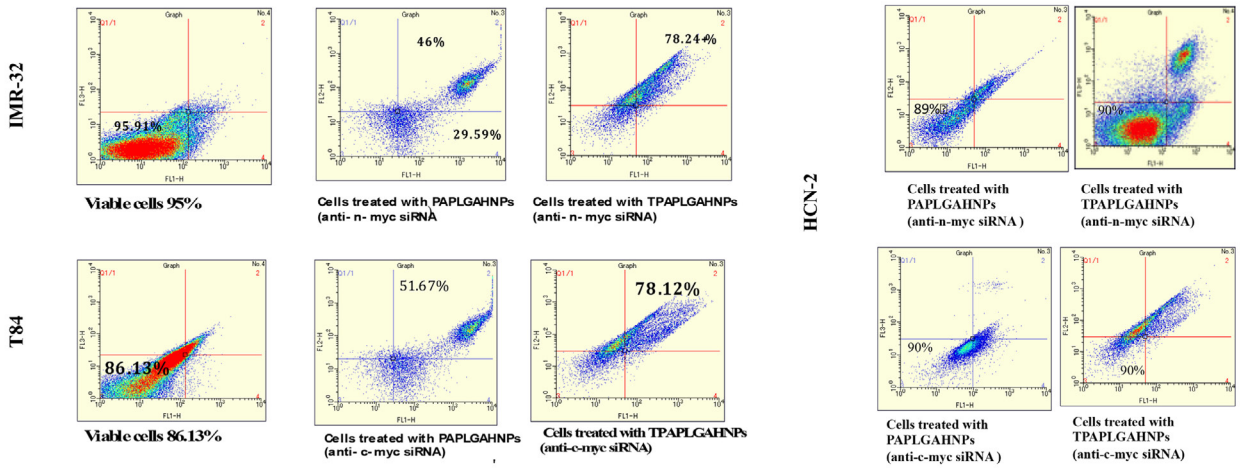

Figure 7: Study of death in cancer and normal cells after overnight treatment with functionalized nanoparticles.

Notes: (A) Flow cytometry of IMR-32 and T84 cancer cells treated with PAPLGAHNPs and TPAPLGAHNPs after overnight incubation.

(B)Flow cytometry of HCN-2 cells treated with functionalized nanoparticles after overnight incubation.

Abbreviation: PAPLGAHNPs- PNA layered on PLGA-siRNA encapsulated hollow nanoparticles, TPAPLGAHNPs- TAT, siRNA, PNA layered on PLGA- siRNA encapsulated hollow nanoparticles.

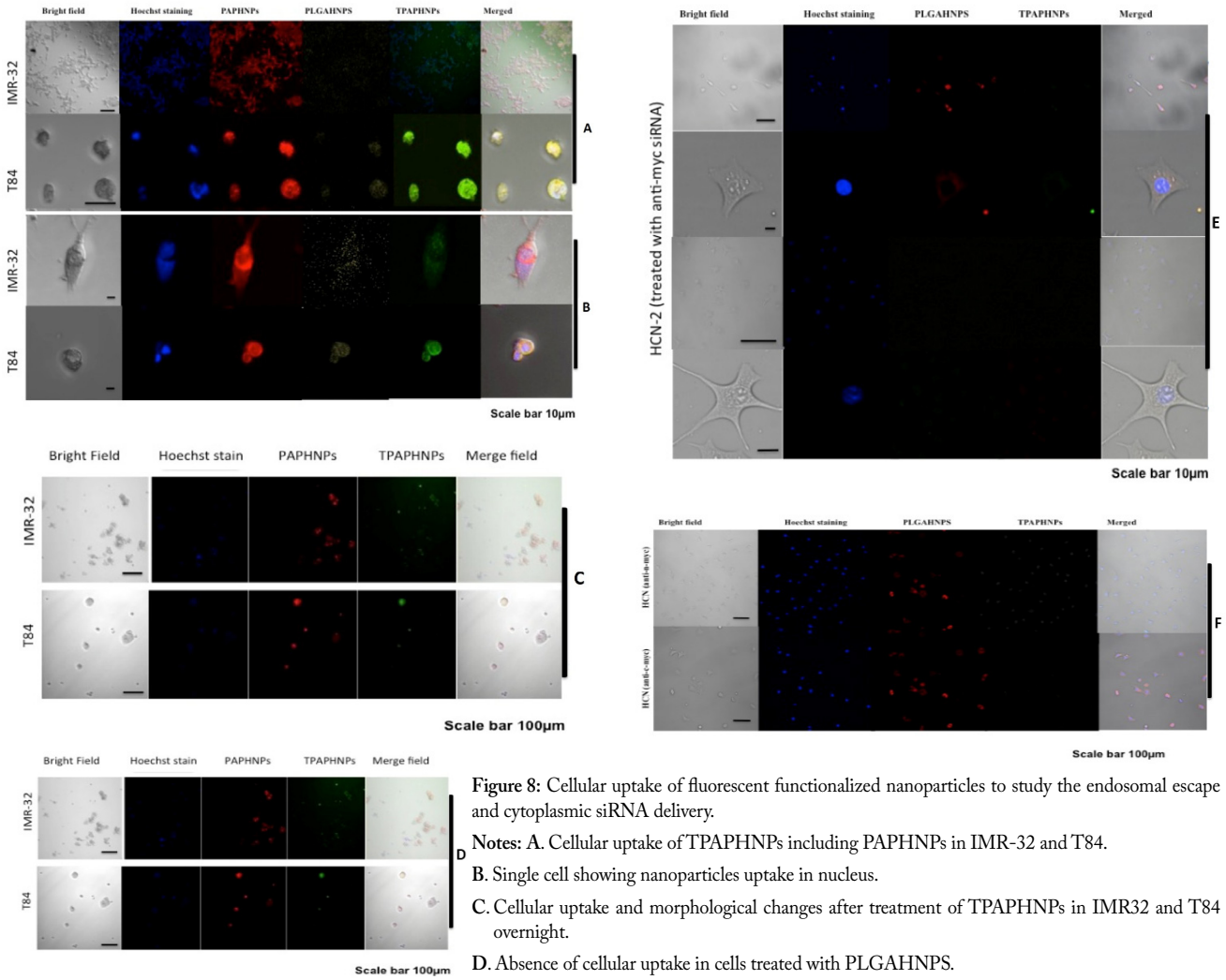

Figure 8: Cellular uptake of fluorescent functionalized nanoparticles to study the endosomal escape and cytoplasmic siRNA delivery.

Notes: A. Cellular uptake of TPAPHNPs including PAPHNPs in IMR-32 and T84.

B. Single cell showing nanoparticles uptake in nucleus.

C. Cellular uptake and morphological changes after treatment of TPAPHNPs in IMR32 and T84 overnight.

D. Absence of cellular uptake in cells treated with PLGAHNPS.

E. Cellular uptake of functionalized nanoparticles in HCN-2 after 4 h.

F. Cellular uptake in normal cells after overnight incubation with functionalized nanoparticles.

Abbreviations: PAPHNPs- PNA-Rhodamine layered on tetrazine PLGA-siRNA encapsulated hollow nanoparticles, TPAPHNPs- TAT-FITC, siRNA, PNA-Rhodamine layered on tartrazine-PLGA- siRNA encapsulated hollow nanoparticles

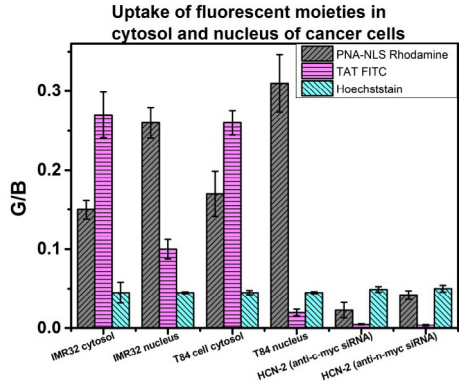

Figure 9: Fluorescent intensity of functionalized nanoparticles after nuclear and cellular uptake.

Notes: Quantification of fluorescent intensity of Rhodamine and FITC after overnight treatment of TPAPHNPs in cytosol and nuclei of cells. Quantification of Hoechst stain in nucleus of the cancer cells.

Abbreviations: PAPHNPs- PNA-Rhodamine layered on tetrazine PLGA-siRNA encapsulated hollow nanoparticles, TPAPHNPs- TAT-FITC, siRNA, PNA-Rhodamine layered on tetrazine-PLGA- siRNA encapsulated hollow nanoparticles

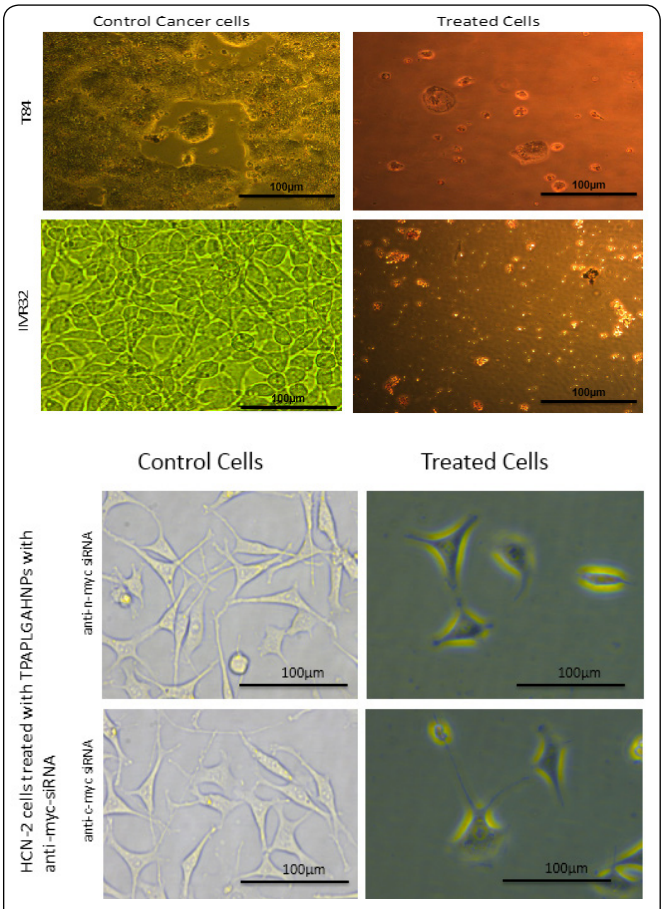

Figure 10: Study of morphological changes in cancer cells.

Notes: Morphological analyses of cancer and normal cells after overnight incubation of TPAPHNPs. No change was observed in normal cells.

Abbreviations: PAPHNPs- PNA-Rhodamine layered on tartrazine PLGA-siRNA encapsulated hollow nanoparticles, TPAPHNPs- TAT-FITC, siRNA, PNA-Rhodamine layered on tetrazine-PLGA- siRNA encapsulated hollow nanoparticles

2 cells with functionalized NPs encapsulated with optimized molar concentration of anti-*MYC*- siRNA ranging from 50 to 250 µg/ml. From figure 6A, C and E we observe the MIC required for inhibiting IMR-32, T84 and HCN-2 cells when treated with functionalized NPs. 200 µg/ml of PAPLGAHNPs and 200 µg/ml of TPAPLGAHNPs was the MIC observed to inhibit IMR-32 cells encapsulated with anti-n-myc siRNA of 70 nM. Also, 250 µg/ml of PAPLGAHNPs and 150 µg/ml of TPAPLGAHNPs was the MIC required to inhibit T84 cells encapsulated with anti-c-myc siRNA of 80 nM. There was no effect on proliferation of HCN-2 when treated with 200 µg/ml of PAPLGAHNPs, 200 µg/ml of TPAPLGAHNPs encapsulated with anti-n-myc siRNA of 70 nM, 250 µg/ml of PAPLGAHNPs and 150 µg/ml of TPAPLGAHNPs encapsulated with anti-c-myc siRNA of 80 nM.

Table 2: Results of flow cytometry represented in percentage cell death in cancer cells after four hours and overnight incubation with functionalized NPs

Sr. No.	Cell Lines	Cell Deaths(%))					
		TPAPLGAHNPs		PAPLGAHNPs		Untreated	
		Overnight	4 h	Overnight	4 h	Overnight	4 h
1	HCN (anti-n-myc siRNA)	10	3	11	2	9	2
2	HCN (anti-c-myc siRNA)	10	4	10	3	9	2
3	IMR-32 (anti-n-myc siRNA)	78.24	67.31	46	9.42	4.09	3
4	T-84 (anti-c-myc siRNA)	78.12	49.12	51.67	12.16	13.83	10.68

Further we performed flow cytometry experiment to determine the effect of functionalized NPs on IMR-32, T84 and HCN-2 cells (Figure 7). The viability of untreated IMR-32, T84 and HCN-2 cells was 96%, 89% and 98% respectively. We observed 67.31% and 49.12% of cellular death in IMR-32 and T84 cells after treatment of TPAPLGAHNPs encapsulated with anti-*MYC*-siRNA after 4 h of incubation. Also, 9.42% and 12.16% of cellular death in IMR-32 and T84 cells after treatment of PAPLGAHNPs encpasulated with anti-*MYC*-siRNA after 4 h of incubation. Treatment of functionalized NPs did not have significant effect on HCN-2 cells (Figure 7B). Also, 78.24% and 78.12% of cellular death was observed in IMR-32 and T84 cells after overnight incubation with TPAPLGAHNPs while 46% and 51.67% of cellular death was observed in IMR-32 and T84 cells after overnight incubation with PAPLGAHNPs encapsulated with anti-*MYC*-siRNA (Figure 7A). There was no effect on HCN-2 cells after overnight incubation with functionalized NPs. The results are tabulated in Table 2

Cellular and nuclear uptake of PAPHNPs and TPAPHNPs

The cellular uptake of two different types of NPs (PAPHNPs and TPAPHNPs) were observed after 4 h of incubation and overnight incubation of NPs with cancer cells and normal cells. The 4 h as well as overnight incubation of NPs showed the presence of fluorescence in cytoplasm and nucleus as observed in figure 8. It is known that the successful endosomal escape is crucial for the siRNA carriers to improve siRNA silencing efficiency [24]. We have observed co-localization of PNA-Rhodamine and Tartrazine-PLGAHNPS in cytoplasm and nucleus of cancer cells by confocal microscopy. Within

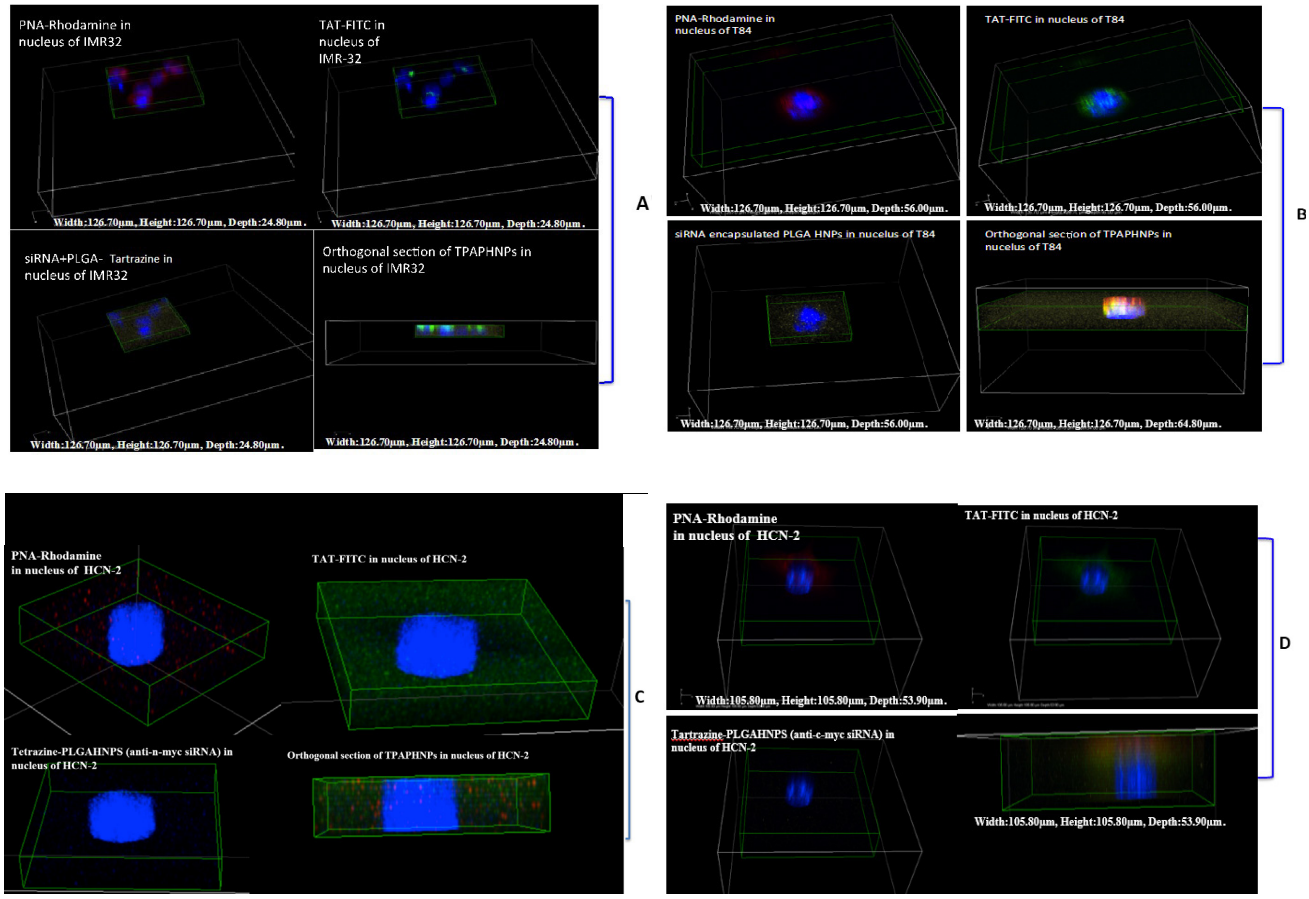

Figure 11: Nucleus uptake of functionalized nanoparticles after four hours of incubation.

Notes: **A.** 3D Images showing nuclear uptake of TPAPHNPs in IMR32 neuroblastoma after 4 h of incubation

B. 3D Images showing nuclear uptake of TPAPHNPs in T84 colorectal carcinoma after 4 h of incubation.

C. 3D images showing nuclear uptake of TPAPHNPs containing anti-c-myc siRNA after 4 h of incubation.

D. 3D images showing nuclear uptake of TPAPHNPs containing anti-n-myc siRNA after 4 h of incubation.

Abbreviations: PAPHNPs- PNA-Rhodamine layered on tartrazine PLGA-siRNA encapsulated hollow nanoparticles, TPAPHNPs- TAT-FITC, siRNA, PNA-Rhodamine layered on tetrazine-PLGA-siRNA encapsulated hollow nanoparticles

4 h of coincubation with PAPHNPs and TPAPHNPs, the NPs were randomly distributed all over the cytoplasm. In figure 8A we have observed co-localization indicating the presence of PNA-Rhodamine, FITC-TAT and Tartrazine-PLGAHNPS in IMR-32 and T84 cells. The single cell uptake as observed in figure 8B of IMR-32 and T84 represents that NPs were present both in cytoplasm and in nucleus. In figure 8C we observed morphological changes in cancer cells after overnight incubation with fluorescent NPs. In figure 8D, cells treated with Tartrazine-PLGAHNPs did not show any cellular or nuclear uptake. According to figure 8E and F cytosol and nuclear uptake of NPs was less in HCN-2 cells. These results suggest the enhanced uptake of NPs in cancer cells.

We have observed that the cells treated with TPAPHNPs showed the uptake of NPs into the nucleus. Moreover, the cells treated with PAPHNPs showed less uptake in nucleus compared to TPAPHNPs. This may be because TAT protects the NPs from external environment. Based on figure 8 quantification of fluorescence intensity was calculated using equation 3 and presented in figure 9. The fluorescence intensity of Rhodamine was less in cells treated with PAPHNPs. In IMR-32 and T84, the presence of FITC in cytosol was high, while less in nucleus. This concluded that TAT helps the PAPHNPs to cross-cellular membrane and release siRNA.

The confocal images in figure 8C and the phase contrast microscopy images in figure 10 revealed that the cellular uptake of TPAPHNPs show morphological changes after the overnight incubation. The TPAPHNPs treated IMR-32 underwent shrinkage and were clumped. We also observed that the IMR-32 cells lost adherence and started floating. We have observed same effect in T84 cells. We observed no adverse effect of NPs on HCN-2 cells. These results clearly prove that the NPs resulted in cancer cell death. Further to confirm nuclear uptake of NPs, cells were treated with TPAPHNPs and were visualized by 3D imaging after 4 h (Figure 11). In figure 11A and B we observed the nuclear uptake and colocalization of PNA-Rhodamine, TAT-FITC and Tartrazine-PLGAHNPS. The nucleus was stained with Hoechst stain. We have observed higher nuclear uptake of PNA conjugated NPs in IMR-32 and T84. The presence of PNA-Rhodamine, Tartrazine-PLGAHNPS in nucleus determined the uptake of NPs through the nuclear membrane. The process of internalization initiates during the first 4 h. In figure 11C and D the orthogonal section of HCN-2 nucleus proved that NPs were completely absent inside the nucleus. From figure 11 we inferred that nuclear uptake of siRNA encapsulated PLGAHNPS were mediated by PNA and TAT.

Effect of NPs on gene expression

To investigate the RNAi efficiency with anti-n-myc and anti-c-myc siRNA, IMR-32 and T84 cells were treated with PAPLGAHNPs and TPAPLGAHNPs and the relative gene expression was studied using qRT-PCR analysis. There was significant down regulation of c-myc and n-myc gene expression. To study the relative gene expression efficacy (Figure 12), cells were incubated with different concentrations of siRNA encapsulated PAPLGAHNPs and TPAPLGAHNPs. IMR-32 cells were incubated with anti-n-myc siRNA (50 nM and 70 nM) and T84 cells were incubated with anti-c-myc siRNA (50 nM and 80 nM). We have observed a decrease in mRNA expression as observed in figure 12. These results suggested 1.2 fold decrease in n-myc expression and 0.6 fold decrease in c-myc mRNA expression. To further investigate the efficiency of gene silencing, qRT-PCR was performed and compared with β2-microglobulin, a housekeeping gene. HCN-2 cells were also treated with same concentration of functionalized NPs and no effect in gene regulation was observed. The relative gene expression was calculated based on equation 4. In IMR-32 cells mRNA expression was reduced from 96.7% to 32.4% and in T84 cells from 74% to 31% when treated with PAPHNPs. On treatment with TPAPHNPs the gene expression in IMR-32 was reduced from 96.7% to 5.64% and in T84 from 74% to 8.815%. These results suggested gene silencing using sequence specific siRNA using PLGAHNPs as delivery vehicle.

Discussion

Recently RNAi therapeutic have emerged as a promising treatment to silence disease-associated genes. Numerous siRNA-based drugs especially, nanoparticle-based treatments are currently undergoing human clinical trials. The siRNA delivery using NPs have to overcome certain limitations like a) proper encapsulation and sustained release, b) escape from RNase degradation, c) targeted delivery, d) cross the cell barrier and cytosolic release, e) bind to RNA induced silencing complex (RISC) and f) renal clearance [48]. Keeping these points in mind we have designed our NPs to overcome these issues. Targeting moieties were attached by LBL assembly to PLGAHNPS. We have demonstrated *in vitro* effect of siRNA encapsulated HNPs in cancer cells.

In our study, siRNA encapsulated PLGAHNPs were functionalized with PNA-NLS, a layer of siRNA and CPP using LBL assembly. Owing to the positive charge of PNA-NLS, the attachment with TAT was difficult. There are chances that the chemical modification of PNA-NLS might result in the reduction of its original activity. CPP was used to increase the cytosolic delivery. Therefore a layer of anti-*MYC* siRNA was added on PAPLGAHNPS, to create a negatively charged particle. Then another layer of CPP (TAT) was added. Thus our NPs were layered by cell penetrating and nucleus penetrating moieties. The size of completely functionalized NPs was 123 ± 0.87 nm. TAT peptide helps NPs to penetrate the cell membrane. As the NPs enter the cytosol the siRNA layer encounters the cytosolic enzyme degradation or may come across the DICER enzyme and degrade mRNA. However

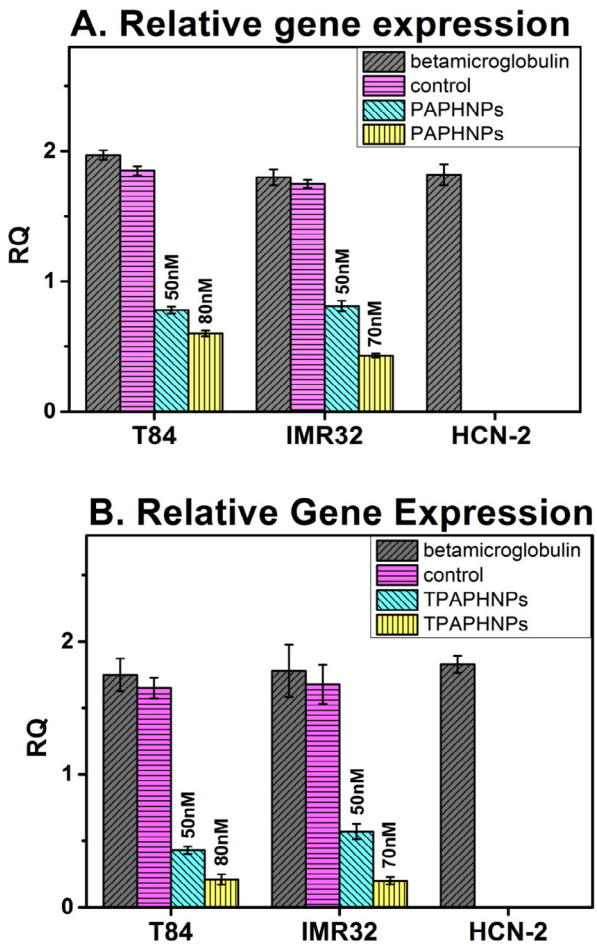

Figure 12: Downregulation of proto-oncogene (MYC) in cancer cells after overnight incubation with functionalized nanoparticles.

Notes: Real-time reverse-transcription polymerase chain reaction was performed and relative gene expression was compared withy that of beta microglobulin.

A) Effect of PAPLGAHNPs on gene expression in IMR 32, T84 and HCN-2 cell lines.

B) Effect of TPAPLGAHNPs on myc gene in IMR 32, T84 and HCN-2 cell lines.

Abbreviations: PAPLGAHNPs- PNA layered on tetrazine PLGA-siRNA encapsulated hollow nanoparticles, TPAPLGAHNPs- TAT, siRNA, PNA-layered on PLGA- siRNA encapsulated hollow nanoparticles

the siRNA encapsulated inside the polymer remains safe due to presence of PNA-NLS. The PNA-NLS further helps in targeting the nucleus and delivering the siRNA. Tonelli et al. reported the penetration of NLS-myc gene complex into the nucleus and had anti-myc effect in cancer cells [49]. The inhibitory effect of *MYC* transcription was highly selective and specific, and had antiproliferative effects in cancer cells. Therefore siRNA encapsulated polymeric NPs was delivered safely into nucleus. Once it enter the nucleus, the PNA-NLS functionalized NP is susceptible to degradation [50]. When polymer is degraded, siRNA is released and results in the downregulation of *MYC* gene. As the siRNA designed is sequence specific it targets the n-myc and c-myc mRNA in IMR-32 and T84 cells respectively. This results in the suppression of *MYC* and downregulates the gene expression resulting in cell death.

Conclusion

In our study, PLGAHNPs were used as nano carrier for anti-*MYC* siRNA delivery. PLGAHNPs were able to encapsulate approximately 2000 µg/ml siRNA. Targeted delivery of anti-*MYC* siRNA encapsulated NPs was achieved using PNA-NLS and TAT. These functionalized NPs resulted in receptor-mediated endocytosis and delivered anti-*MYC* siRNA in endolysosomal compartments. Down regulation of gene was observed due to efficient delivery of siRNA in the targeted cells. The targeted siRNA could be further applied to other disease associated genes and could be used for *in vivo* applications. Thus, the combination of PLGA HNPs, TAT, and PNA-NLS to formulate nanocarriers provides an attractive strategy for siRNA delivery in therapeutic use. In addition, there are several ways for incorporating diagnostic and therapeutic agents into cancer cells such as protein modification, surface loading and core loading. Since the interaction between TAT, PNA-NLS and siRNA is based on surface loading, the core siRNA still can be replaced with other drugs for treatment or image-guided therapy. This system can be extended to other NPs or peptide-based delivery systems for creating safe and effective therapeutic delivery.

References

1. Dorn G, Patel S, Wotherspoon G, Hemmings-Mieszczak M, Barclay J, et al. 2004. siRNA relieves chronic neuropathic pain. *Nucleic Acids Res* 32(5): e49. doi: 10.1093/nar/gnh044
2. Kim SH, Jeong JH, Lee SH, Kim SW, Park TG. 2008. Local and systemic delivery of VEGF siRNA using polyelectrolyte complex micelles for effective treatment of cancer. *J Control Release* 129(2): 107–116. doi: 10.1016/j.jconrel.2008.03.008
3. Lee H, Kim SI, Shin D, Yoon Y, Choi TH, et al. 2009. Hepatic siRNA delivery using recombinant human apolipoprotein A-I in mice. *Biochem Biophys Res Commun* 378(2): 192-196. doi: 10.1016/j.bbrc.2008.11.029
4. Novina CD, Sharp PA. 2004. The RNAi revolution. *Nature* 430(6996): 161–164. doi:10.1038/430161a
5. Fire A, Xu S, Montgomery MK, Kostas SA, Driver SE, et al. 1998. Potent and specific genetic interference by double-stranded RNA in Caenorhabditis elegans. *Nature* 391(6669): 806-811. doi:10.1038/35888
6. McCaffrey AP, Meuse L, Pham TT, Conklin DS, Hannon GJ, et al. 2002. RNA interference in adult mice. *Nature* 418(6893): 38–39. doi:10.1038/418038a
7. Kamimura K, Suda T, Zhang G, Liu D. 2011. Advances in Gene Delivery Systems. *Pharmaceut Med* 25(5): 293-306. doi: 10.1007/BF03256872
8. Kay MA, Glorioso JC, Naldini L. 2001. Viral vectors for gene therapy: the art of turning infectious agents into vehicles of therapeutics. *Nat Med* 7(1): 33-40. doi: 10.1038/83324
9. Luo D, Saltzman WM. 2000. Synthetic DNA delivery systems. *Nat Biotechnol* 18(1): 33-37. doi:10.1038/71889
10. Saul JM, Linnes MP, Ratner BD, Giachelli CM, Pun SH. 2007. Delivery of non-viral gene carriers from sphere-templated fibrin scaffolds for sustained transgene expression. *Biomaterials* 28(31): 4705-4716. doi:10.1016/j.biomaterials.2007.07.026
11. Semple SC, Akinc A, Chen J, Sandhu AP, Mui BL, et al. 2010. Rational design of cationic lipids for siRNA delivery. *Nat Biotechnol* 28(2): 172-176. doi: 10.1038/nbt.1602
12. Yano J, Hirabayashi K, Nakagawa S, Yamaguchi T, Nogawa M, et al. 2004. Antitumor activity of small interfering RNA/cationic liposome complex in mouse models of cancer. *Clin Cancer Res* 10(22): 7721-7726. doi: 10.1158/1078-0432.CCR-04-1049
13. Gary DJ, Puri N, Won YY. 2007. Polymer-based siRNA delivery: perspectives on the fundamental and phenomenological distinctions from polymer-based DNA delivery. *J Control Release* 121(1-2): 64-73. doi:10.1016/j.jconrel.2007.05.021
14. Alam MR, Dixit V, Kang H, Li ZB, ChenX, et al. 2008. Intracellular delivery of an anionic antisense oligonucleotide via receptor-mediated endocytosis. *Nucleic Acids Res* 36(8): 2764-2776. doi: 10.1093/nar/gkn115
15. Ariga K, Hill JP, Ji Q. 2007. Layer-by-layer assembly as a versatile bottom-up nanofabrication technique for exploratory research and realistic application. *Phys Chem Chem Phys* 9(5): 2319-2340. doi: 10.1039/B700410A
16. Elbakry A, Zaky A, Liebl R, Rachel R, Goepferich A, et al. 2009. Layer-by-layer assembled gold NPs for siRNA delivery. *Nano Lett* 9: 2059-2064. doi: 10.1021/nl9003865
17. Qi L, Gao X. 2008. Quantum dot-amphipol nanocomplex for intracellular delivery and real-time imaging of siRNA. *ACS Nano* 2(7): 1403-1410. doi: 10.1021/nn800280r
18. Soutschek J, Akinc A, Bramlage B, Charisse K, Constien R, et al. 2004. Therapeutic silencing of an endogenous gene by systemic administration of modified siRNAs. *Nature* 432(7014): 173-178. doi:10.1038/nature03121
19. Audouy SA, de Leij LF, Hoekstra D, Molema G. 2002. In vivo characteristics of cationic liposomes as delivery vectors for gene therapy. *Pharm Res* 19(11): 1599-1605. doi: 10.1023/A:1020989709019
20. Ma Z, Li J, He F, Wilson A, Pitt B, et al. 2005. Cationic lipids enhance siRNA-mediated interferon response in mice. *Biochem Biophys Res Commun* 330(3): 755-759. doi:10.1016/j.bbrc.2005.03.041
21. Rao NM. 2010. Cationic lipid-mediated nucleic acid delivery: beyond being cationic. *Chem Phys Lipids* 163(3): 245-252. doi: 10.1016/j.chemphyslip.2010.01.001
22. Cho WS, Cho M, Jeong J, Choi M, Cho HY, et al. 2009. Acute toxicity and pharmacokinetics of 13 nm-sized PEG-coated gold NPs. *Toxicol Appl Pharmacol* 236(1): 16-24. doi: 10.1016/j.taap.2008.12.023
23. Geys J, Nemmar A, Verbeken E, Smolders E, Ratoi M, et al. 2008. Acute toxicity and prothrombotic effects of quantum dots: impact of surface charge. *Environ Health Perspect* 116(12): 1607-1613. doi: 10.1289/ehp.11566
24. Alexis F, Pridgen E, Molnar LK, Farokhzad OC. 2008. Factors affecting the clearance and biodistribution of polymeric NPs. *Mol Pharm* 5(4): 505-515. doi: 10.1021/mp800051m
25. Whitehead KA, Langer R, Anderson DG.2009. Knocking down barriers: advances in siRNA delivery. *Nat Rev Drug Discov* 8(2): 129-138. doi: 10.1038/nrd2742
26. Lee JM, Yoon TJ, Cho YS. 2013. Recent developments in nanoparticle-based siRNA delivery for cancer therapy. *Biomed Res Int* 2013: 782041. doi: 10.1155/2013/782041
27. Inoue T, Sugimoto M, Sakurai T, Saito R, Futaki N, et al. 2007. Modulation of scratching behavior by silencing an endogenous cyclooxygenase-1 gene in the skin through the administration of siRNA. *J Gene Med* 9(11): 994-1001. doi: 10.1002/jgm.1091
28. Patil Y, Panyam J. 2009. Polymeric NPs for siRNA delivery and gene silencing. *Int J Pharm* 367(1-2): 195-203. doi: 10.1016/j.ijpharm.2008.09.039
29. Raichur A, Nakajima Y, Nagaoka Y, Maekawa T, Kumar DS. 2014. Hollow polymeric (PLGA) nano capsules synthesized using solvent emulsion evaporation method for enhanced drug encapsulation and release efficiency. *Materials Research Express* 1: 1-15. doi:10.1088/2053-1591/1/4/045407
30. Ui-Tei K, Naito Y, Takahashi F, Haraguchi T, Ohki-Hamazaki H, et al. 2004. Guidelines for the selection of highly effective siRNA sequences for mammalian and chick RNA interference. *Nucleic Acids Res* 32(3): 936-948. doi: 10.1093/nar/gkh247

31. Cun D, Jensen DK, Maltesen MJ, Bunker M, Whiteside P, et al. 2011. High loading efficiency and sustained release of siRNA encapsulated in PLGA NPs: quality by design optimization and characterization. *Eur J Pharm Biopharm* 77(1): 26-35. doi: 10.1016/j.ejpb.2010.11.008
32. Katas H, Raja MA, Lam KL. 2013. Development of Chitosan NPs as a Stable Drug Delivery System for Protein/siRNA. *Int J Biomater* 2013: 146320. doi: 10.1155/2013/146320
33. Shimanovich U, Munder A, Loureiro A, Azoia NG, Gomes A, et al. 2014. Gene Silencing by siRNA NPs Synthesized via Sonochemical Method. *J Nanomed Nanotechnol* 5(3): 1000204. doi: 10.4172/2157-7439.1000204
34. Caputo A, Brocca-Cofano E, Castaldello A, De Michele R, Altavilla G, et al. 2004. Novel biocompatible anionic polymeric microspheres for the delivery of the HIV-1 Tat protein for vaccine application. *Vaccine* 22(21-22): 2910-2924. doi:10.1016/j.vaccine.2003.12.025
35. Moschos SA, Jones SW, Perry MM, Williams AE, Erjefalt JS, et al. 2007. Lung delivery studies using siRNA conjugated to TAT(48-60) and penetratin reveal peptide induced reduction in gene expression and induction of innate immunity. *Bioconjug Chem* 18(5): 1450-1459. doi: 10.1021/bc070077d
36. Gullotti E, Park J, Yeo Y. 2013. Polydopamine-based surface modification for the development of peritumorally activatable NPs. *Pharm Res* 30(8): 1956-1967. doi: 10.1007/s11095-013-1039-y
37. Arango D, Mariadason JM, Wilson AJ, Yang W, Corner GA, et al. 2003. c-Myc overexpression sensitises colon cancer cells to camptothecin-induced apoptosis.*Br J Cancer* 89(9): 1757-1765. doi:10.1038/sj.bjc.6601338
38. Judware R, Lechner R, Culp LA. 1995. Inverse expressions of the N-myc oncogene and beta 1 integrin in human neuroblastoma: relationships to disease progression in a nude mouse model system. *Clin Exp Metastasis* 13(2): 123-133. doi: 10.1007/BF00133617
39. Shen J, Kim HC, Su H, Wang F, Wolfram J, et al. 2014. Cyclodextrin and polyethylenimine functionalized mesoporous silica NPs for delivery of siRNA cancer therapeutics. *Theranostics* 4(5): 487-497. doi: 10.7150/thno.8263
40. Laroui H, Geem D, Xiao B, Viennois E, Rakhya P, et al. 2014. Targeting Intestinal Inflammation with CD98 siRNA/PEI–loaded NPs. *Molecular Therapy* 22(1): 69–80. doi:10.1038/mt.2013.214
41. Kabilova TO, Chernolovskaya EL, Vladimirova AV, Vlassov VV. 2006. Inhibition of human carcinoma and neuroblastoma cell proliferation by anti-c-myc siRNA. *Oligonucleotides* 16(1): 15-25. doi:10.1089/oli.2006.16.15
42. Costa EC, Gaspar VM, Marques JG, Coutinho P, Correia IJ. 2013. Evaluation of nanoparticle uptake in co-culture cancer models. *PLoS One* 8(7): e70072. doi: 10.1371/journal.pone.0070072
43. Jin H, Lovell JF, Chen J, Lin Q, Ding L, et al. 2012. Mechanistic insights into LDL nanoparticle-mediated siRNA delivery.*Bioconjug Chem* 23(1): 33-41. doi: 10.1021/bc200233n
44. Keum CG, Noh YW, Baek JS, Lim JH, Hwang CJ, et al. 2011. Practical preparation procedures for docetaxel-loaded NPs using polylactic acid-co-glycolic acid. *Int J Nanomedicine* 6: 2225-2234. doi: 10.2147/IJN.S24547
45. Singha K, Namgung R, Kim WJ. 2011. Polymers in Small Interfering RNA Delivery. *Oligonucleotides*. 21: 133-147
46. Scherphof GL. 1991. *Targeted Drug Delivery*. 285–313.
47. Gullotti E, Yeo Y. 2012. Beyond the imaging: limitations of cellular uptake study in the evaluation of NPs. *J Control Release* 164(2): 170-176. doi: 10.1016/j.jconrel.2012.04.042
48. Gilleron J, QuerbesW, Zeigerer A, Borodovsky A, Marsico G, et al. 2013. Image-based analysis of lipid nanoparticle–mediated siRNA delivery, intracellular trafficking and endosomal escape. *Nature biotechnology* 31(7): 638–646. doi:10.1038/nbt.2612
49. Tonelli R, McIntyre A, Camerin C, Walters ZS, Di Leo K, et al. 2012. Antitumor activity of sustained N-myc reduction in rhabdomyosarcomas and transcriptional block by antigene therapy. *Clin Cancer Res* 18(3): 796-807. doi: 10.1158/1078-0432.CCR-11-1981
50. Cutrona G, Carpaneto EM, Ulivi M, Roncella S, Landt O, et al. 2000. Effects in live cells of a c-myc anti-gene PNA linked to a nuclear localization signal. *Nat Biotechnol*18(3): 300-303. doi:10.1038/73745